Tunable erbium–ytterbium fiber sliding-frequency soliton laser

M. Romagnoli and S. Wabnitz

Fondazione Ugo Bordoni, Via B. Castiglione 59, 00142 Rome, Italy

P. Franco and M. Midrio

Dipartimento di Elettronica e Informatica, Università di Padova, Via G. Gradenigo 6/A, 35131 Padova, Italy

F. Fontana

Pirelli Cavi s.p.a., Viale Sarca 202, 20146 Milano, Italy

G. E. Town

Sydney University Electrical Engineering, Sydney University, New South Wales 2006, Sydney, Australia

Received March 31, 1994; revised manuscript received July 6, 1994

We characterize the soliton-train emission from an Er–Yb-doped fiber loop laser. We discuss the self-starting dynamics and pulse-repetition-rate control in this sliding-frequency soliton laser. We show that the laser truly self-starts after only one cavity round trip. In the steady state the laser emits a closely spaced train of solitons. We also show that the output pulse width may be controlled by the interplay of continuous frequency shifting, bandwidth-limited amplification, and nonlinear polarization rotation of the circulating solitons. The repetition rate is fixed by means of a weak intracavity feedback. The laser is tunable by shifting of the filter wavelength through the whole spectral band of the active fiber.

1. INTRODUCTION

The most commonly used technique for the generation of short optical pulses is active or passive locking of the longitudinal modes of a laser cavity. Nevertheless, phase locking the cavity modes requires accurate control of the laser parameters. For instance, in actively mode-locked lasers the modulation frequency and the cavity fundamental frequency should typically match within 10–100 Hz. In fiber lasers the interplay of group-velocity dispersion and self-phase modulation leads to soliton shaping[1,2] and temporal compression of the output pulses.

Short optical pulses may also be generated by continuously shifting of the frequency of the light that circulates inside an active ring laser.[3] Frequency shifting suppresses the longitudinal modes of the cavity. This strongly increases the threshold for the cw operation of the laser. On the other hand, a relatively low threshold may be seen for short pulses as a consequence of the combined action of frequency shifting and spectral reshaping induced by nonlinear spectral broadening and filtering.[4] With average anomalous intracavity dispersion, stable pulsing may occur in the form of optical solitons.[5,6] In this case theory[5] predicts that the output pulse width depends only on the filter bandwidth and the single-pass frequency shift and is independent of the emission wavelength, the dispersion, and the length of the cavity. Moreover, high repetition rates (as high as 20 GHz, Ref. 5) result from the cancellation of soliton interactions.[6,7] Note the analogy of the present technique with the sliding-filter method that was proposed for stabilizing soliton transmissions.[8] In the sliding-filter technique the center frequency of the filter is adiabatically shifted along the transmission line. In this way the link is effectively transparent for solitons but opaque for noise. In a complementary way one may keep the filter center frequency fixed and continuously shift the frequency of the signal. Clearly this produces the same effect as sliding the central frequency of the guiding filter, with the advantage that this method is applicable to recirculating loops used as optical storage rings or fiber lasers.

In this paper we first investigate the transient dynamics in the sliding-frequency soliton laser, and we show the process of short-pulse formation. We differentiate two different regimes of operation, depending on whether there is a harmonic relationship between the frequency shift provided by the acousto-optic modulator (AOM) and the fundamental frequency of the cavity. In the resonant condition the sequences of pulses initially develop as expected in harmonic mode locking. In the more common nonresonant situation long square-shaped envelopes of closely spaced pulses appear. In either regime the duration of the individual solitons in the sequence is the same.

We also present here a theoretical analysis, based on soliton perturbation theory, of the pulse-shortening action of fast saturable absorption (or nonlinear gain[9,10]) in a sliding-frequency soliton laser. We experimentally confirm that nonlinear polarization rotation in a sliding-frequency Er–Yb-doped fiber soliton laser may reduce the output pulse width. On the other hand, we show

0740-3224/95/010072-05$06.00

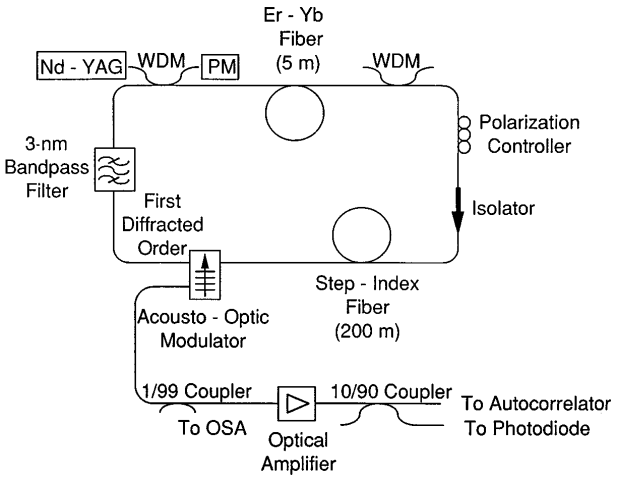

Fig. 1. Schematic of the experimental setup. PM, powermeter.

that the maximum repetition rate corresponding to a soliton separation of 3.4 pulse widths at half-power is achieved as a consequence of the suppression of the soliton–soliton interaction that is a characteristic of the sliding-frequency systems.[8] Moreover, we show that tuning the laser wavelength throughout the whole gain bandwidth leaves the output pulse width unchanged.

2. EXPERIMENTAL APPARATUS

It is convenient to introduce first the experimental setup of the sliding-frequency soliton laser that is depicted in Fig. 1. This facilitates the understanding of the theoretical treatment in Section 3. In the present experiment the active medium was a 10-m-long Er–Yb-doped fiber, whereas in the previous experiment we used an Er-doped fiber.[5] The Er–Yb-doped fiber was pumped with 1 W of cw power from a Nd:YAG laser emitting at $\lambda_{\text{pump}} = 1064$ nm. The doped fiber absorption at λ_{pump} was 1 dB/m. The pump power was coupled in and out of the active fiber by two dichroic couplers (wavelength division multiplexers, WDM's). After calibration the radiation leaking from the output of the first WDM was sent to a powermeter. The frequency shifter was a traveling-wave bulk AOM whose frequency could be finely tuned by means of a sine-wave synthetizer in the range of 69–87 MHz. In the present geometry the AOM induces a frequency downshift. A 3-nm-wide bandpass filter was used for spectral reshaping. The center wavelength of the filter could be tuned in the range of 1520–1580 nm. Unidirectional operation of the laser was ensured by a polarization-insensitive isolator. The intracavity polarization controller allowed us to adjust the output pulse width. We added to the loop 210 m of step-index fiber to control the value of the average frequency-sliding rate. With a total loop length of 240 m, the average group-velocity dispersion was $\beta_2 = -16.5$ ps^2/km. The first diffracted order of the AOM was coupled into the fiber ring, whereas the zeroth order was used as output coupler. The laser output was equally split by a 3-dB coupler and was sent either to an optical powermeter or to spectral and temporal detection units. The spectrum was monitored by an optical spectrum analyzer (OSA) after an additional splitting from a 1:99 coupler. The light emerging from the 99% port of the coupler was first amplified by an optical amplifier module and then split between an autocorrelator (90%) and a fast photodiode (10%).

3. THEORY

Consider first nonlinear pulse propagation in a continuously frequency-shifted active fiber loop with filtering and fast saturable absorption (see Fig. 1). By distributing the various elements in the loop, one obtains the averaged equation[6]

$$\frac{\partial u}{\partial Z} - \frac{i}{2}\frac{\partial^2 u}{\partial T^2} - i|u|^2 u - i\alpha_0 T u = \delta u + V_f \frac{\partial u}{\partial T} + \beta\frac{\partial^2 u}{\partial T^2} + \gamma|u|^2 u\,. \quad (1)$$

Here T and Z are the dimensionless time and distance, α is the frequency-shifting rate, δ is the cw gain, and V_f and β are the filter-induced group-velocity shift and dispersion, respectively. The nonlinear gain parameter γ describes the equivalent fast-saturable-absorber mechanism that is induced by a polarization-dependent cavity loss. Note that Eq. (1) may be used to show the equivalence[6] between the present sliding-light technique and the sliding-filter method.[7,8] By neglecting the inessential group-velocity shift V_f, one may analyze the effects of both linear filtering as perturbations to the one-soliton solution of Eq. (1) $\beta = \delta = \gamma = 0$ (Ref. 11):

$$u(T, Z) = \eta\ \text{sech}\{\eta[t - \xi(Z)]\}\exp[i\kappa(Z)T + i\psi(Z)],$$

where $\xi = \alpha Z^2/2$ is the soliton position, $\kappa = \mathrm{d}\xi/\mathrm{d}z = \alpha Z$ is its frequency, and $\mathrm{d}\psi/\mathrm{d}Z = (\eta^2 - \kappa^2)/2$. In the presence of bandwidth-limited amplification and nonlinear gain, perturbation theory[6,7,10] yields for the evolution of the soliton amplitude η and frequency κ

$$\frac{\mathrm{d}\eta}{\mathrm{d}Z} = 2\delta\eta - 2\beta\eta\left(\frac{\eta^2}{3} + \kappa^2\right) + \frac{4}{3}\gamma\eta^3\,, \quad (2.a)$$

$$\frac{\mathrm{d}\kappa}{\mathrm{d}Z} = \alpha - \frac{4}{3}\beta\eta^2\kappa\,. \quad (2.b)$$

From Eq. (2.b) one obtains that in the steady state (i.e., for $\mathrm{d}\eta/\mathrm{d}Z = \mathrm{d}\kappa/\mathrm{d}Z = 0$) the soliton frequency shift from the peak gain value is $\kappa_f = 3\alpha/(4\beta\eta^2)$. The steady-state value of the soliton time width may be found from Eqs. (2) when the value of the cw gain δ is minimized with respect to η. This implies, on the one hand, the minimum threshold condition for the laser. On the other hand, reducing the cw gain increases the stability of periodically amplified solitons.[9]

In real units, $\Delta\Omega$ is the filter bandwidth (2π terahertz), β_2 is the fiber group-velocity dispersion (picoseconds squared per kilometer), $T_{\text{FWHM}} = 1.763\tau$ is the soliton FWHM pulse width (picoseconds), $L_D = \tau^2/\beta_2$ is the dispersion length (kilometers), Z_A is the loop length (kilometers), Δf is the net AOM frequency shift (megahertz), P_0 is the soliton peak power (watts), and γ_1 is the nonlinear gain coefficient (inverse watts per kilometer). One

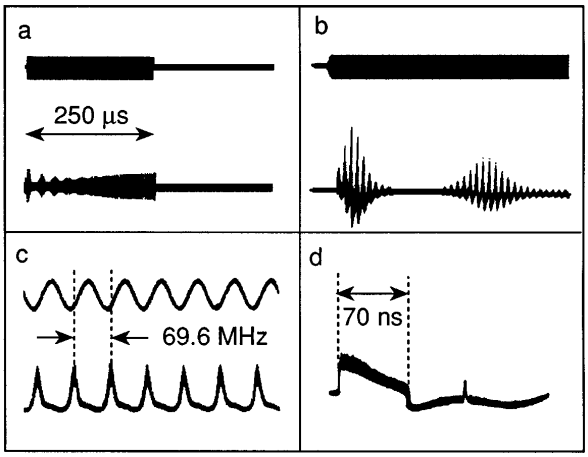

Fig. 2. Transient dynamics of the sliding-frequency soliton laser. a–c, Resonant case. a, The upper trace is the rf signal, and the lower trace is the optical signal whose modulation depends on the relaxation oscillation; b, enlarged detail of a: here it is shown that an envelope is formed after the first round trip of the radiation in the cavity; c, expansion of one of the envelopes shown in b. d, Nonresonant case: the square-shaped envelope consists of a long sequence of closely spaced solitons; the width of the envelope increases while the pump power is increased.

obtains, for the parameters in Eq. (1), the folllowing expressions:

$$\alpha = \frac{(2\pi 10^{-6})\Delta f \tau^3}{Z_A \beta_2}, \qquad \beta = \frac{2L_D}{\Delta\Omega^2 Z_A \tau^2},$$
$$\gamma = \gamma_1 P_0 L_D, \tag{3}$$

whereas the time width of the pulses from the laser τ, obeys

$$\left[\frac{27}{8}\frac{(2\pi 10^{-6})^2 \Delta f^2 \Delta\Omega^4}{4}\right]\tau^6 + (\gamma_1 P_0 \Delta\Omega^2 Z_A)\tau^2 = 1. \tag{4}$$

Note that without nonlinear gain (i.e., with $\gamma_1 = 0$), the pulse width τ does not depend on Z_A and β_2.[5] Another interesting observation is that the minimization condition that leads to Eq. (4) also corresponds to operating the laser exactly at the critical sliding rate $\alpha = \alpha_c$.[7,8] Recall that α_c is the maximum frequency-sliding rate that still permits the stable trapping of the soliton by the filter. In fact, by linearization of Eqs. (2) one obtains

$$\alpha_c = \pm\beta\left[\frac{8}{27}\left(1 - 2\frac{\gamma}{\beta}\right)\right]^{1/2},$$
$$\kappa_c = \pm\left[\frac{1}{6}\left(1 - 2\frac{\gamma}{\beta}\right)\right]^{1/2}, \tag{5}$$

where the plus or minus refers to the upshift or the downshift operation. By assuming $\alpha = \alpha_c$ in Eq. (5) and by using the real units [Eqs. (3)], one again obtains Eq. (4).

Note that the above expressions are valid for $\beta \geq 2\gamma$: for $\beta = 2\gamma$, $\alpha_c = 0$, and $\kappa_c = 0$. Moreover, note that the continuous frequency shifting of the low-intensity light outside the filter bandpass permits stable operation of the laser in spite of the fact that, for $\kappa = \kappa_c$ and for $d\eta/dZ = 0$ [see Eq. (2.a)], $2\delta = \beta - 2\gamma > 0$. On the other hand, whenever $\alpha = 0$ the pulse stability of a passively mode-locked laser requires that the cw gain δ be less than 0.[9] Clearly this greatly facilitates the startup of the present soliton laser with respect to the conventional passive mode-locking case.

4. EXPERIMENTAL RESULTS AND DISCUSSION

The transient dynamics in the laser was investigated by applying an on–off amplitude modulation (AM) to the rf signal driving the AOM, thereby modulating the loss in the cavity. In this experiment the pump level was constant and the AM frequency was 2 kHz. Figure 2 shows the laser transient response on several time scales. Half a period of the AM modulation applied to the rf drive is shown in the upper trace of Fig. 2a. Following turn-on of the rf drive signal, the active medium population was forced into relaxation oscillations that are shown in the lower trace of Fig. 2a. It is evident that after a few periods of the relaxation oscillations the laser evolves toward the stationary state. It was found that the period of the relaxation oscillations varied with the square root of the pump power, in agreement with the theory developed for a three-level system. Figure 2b is an enlarged detail of the previous figure and shows two periods of the relaxation oscillation. It can be seen that the relaxation oscillation contains a finer periodic structure with an initial delay and period equal to the cavity round-trip time, $T_{rt} = 1.2\ \mu s$. This indicates the formation of temporal features after only one round trip of radiation in the cavity and corresponds to self-starting of the laser. The lower trace in Fig. 2c shows the internal structure of one peak within the envelope of Fig. 2b, with the rf drive signal shown above it for reference. This trace was obtained with the rf drive frequency (i.e., the AOM frequency shift) finely tuned to equal the eighty-fourth harmonic of the cavity fundamental frequency. It can be seen that under these conditions a regular train of pulses is formed with spacing equal to the rf drive period, as in harmonic mode locking. It must be pointed out that the AOM frequency matching to the eighty-fourth harmonic of the cavity fundamental frequency was 69.9 ± 0.04 MHz. The tolerance in the frequency matching is 3 orders of magnitude larger than in harmonic mode locking. The harmonic regime of operation of the laser and the tolerance in the choice of the drive frequency is as predicted by the theory of linear pulse formation in cavities containing an intracavity frequency shifter.[3] Because of the fiber nonlinearity and anomalous dispersion each of the pulses in Fig. 2c develops yet finer structure, breaking up into groups of solitons. On detuning of the rf drive signal from cavity resonance, the field in the cavity self-organizes in the form of long square-shaped envelopes, as illustrated in Fig. 2d. The situation of Fig. 2d is more commonly observed in practice because it does not require adjustment of the rf drive frequency at all. We found that the square-shaped envelopes are composed of a train of solitons. The duration of the square envelope increases with the pump power until it appears that the entire cavity is filled, if sufficient pump power is supplied. Note that in the nonresonant case the soliton repetition rate is asynchronous with the loop round-trip time. This effect is more evident for $\Delta T_{rt} \sim 1$.[3]

The autocorrelation trace of Fig. 3 shows the regular sequence of pulses. In this measurement the center wave-

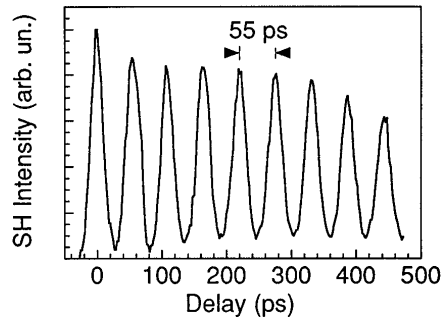

Fig. 3. Long-scan autocorrelation trace of the train of pulses circulating in the laser. SH, second harmonic.

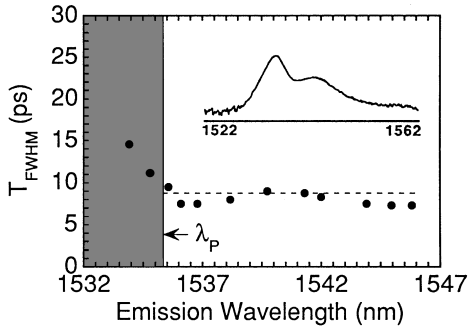

Fig. 4. Pulse width versus laser emission wavelength. The inset shows the spontaneous emission spectrum of the Er–Yb-doped fiber. The shaded region indicates the region in which the cavity bandwidth also depends on the gain spectral shape. This explains the increase in pulse width, $\lambda < \lambda_p$. The dashed line is obtained with $1.763\tau = 8.1$ ps, $\alpha = 0.011$, $\beta = 0.087$, and nonlinear gain coefficient $\gamma = 0.032$.

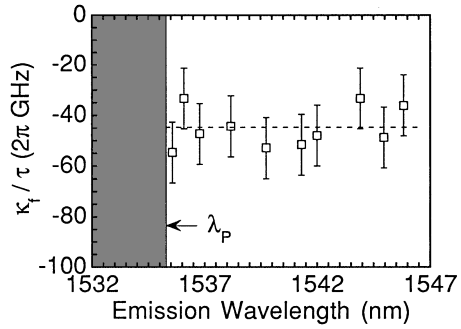

Fig. 5. Soliton equilibrium frequency versus laser emission wavelength. The negative sign of the soliton frequency is due to the frequency downshift induced by the AOM. The fitting curve is obtained with the assumption $\kappa_f = \kappa_c$ and with the same choice of parameters as in Fig. 3.

length of the bandpass filter was set to $\lambda = 1535.3$ nm. The trace of Fig. 3 shows that the single pulse duration (assuming a sech^2 profile) was $T_{\mathrm{FWHM}} = 16$ ps, whereas the separation between any two adjacent pulses was $\Delta\tau = 55$ ps (repetition rate of 18.2 GHz). Note that both pulse duration and separation remain roughly constant throughout the 0.5-ns scan of the autocorrelator. In dimensionless form the observed pulse separation $\Delta = \Delta\tau/\tau = 6$ is the minimum value of separation that still permits the suppression of soliton interactions by frequency sliding.[8]

We measured the wavelength dependence, as shown in Fig. 4, of the minimum value of the output pulse duration throughout the whole bandwidth of the Er–Yb fiber gain spectrum. As soon as the pump power was turned on, the duration of the pulses from the laser easily matched the theoretical prediction [Eq. (4)] with $\gamma = 0$, thus indicating that the laser spontaneously chose the critical-sliding-rate condition, i.e., the minimum excess gain. Note that in the case of sliding-filter soliton transmission lines the value of the ratio may be $\alpha/\beta \le (8/27)^{1/2}$; for instance, in Ref. 7 the ratio $\alpha/\beta = 1/3$. However, in the laser only after an accurate adjustment of the intracavity polarization controller could the pulse durations also be reduced to the values of Fig. 4, and the time–bandwidth product was 0.32 ± 0.1 for all the emission wavelengths. The polarization dependence of the cavity loss combined with the fiber nonlinearity leads to the equivalent fast-saturable-absorber action[10] and most likely originates from the anisotropic Fresnel reflections at the faces of the bulk AOM crystal. In the inset of Fig. 4 we show the emission spectrum of the Er–Yb fiber. The range of tunability of the laser (1534–1548 nm) corresponds to the width of the emission spectrum, which is narrower in this Er–Yb fiber with respect to erbium fibers. As can be seen in Eq. (4), the main factor in determining the laser pulse width is the filter bandwidth. In the wavelength region above the peak gain value $\lambda_p = 1535.3$ nm the emission spectrum is nearly constant, so that the cavity bandwidth is determined only by the filter (in this case we estimate from Eq. (4) that $\beta = 0.087$, which is smaller than the value $\beta = 0.3$ used by Mollenaer *et al.*[7] in the case of sliding-filter soliton transmission. For $\lambda > \lambda_p$ the pulse width ranges between 7 and 8.5 ps. When the nonlinear gain contribution $\gamma = 0.032$ is included, Eq. (4) yields a theoretical value, determined from the assumption that the laser operates at the critical sliding rate of 8.1 ps. Figure 4 shows that whenever $\lambda < \lambda_p$ the effective cavity bandwidth narrows, i.e., $\beta(\lambda < \lambda_p) > \beta(\lambda > \lambda_p)$, and according to Eq. (4) an increase of the pulse width is observed. Figure 5 shows the equilibrium frequency of the soliton propagating in the sliding-frequency system. As expected, the soliton spectrum is downshifted with respect to the filter central frequency. This measurement was achieved by rapid modulation of the amplitude of the rf signal driving the AOM. In this condition the laser did not reach the stationary regime, and the emission wavelength was equal to the filter central wavelength. On the other hand, whenever the AM was turned off, the laser could reach the stationary regime, and the emission shifted toward the equilibrium wavelength. This frequency shift corresponds to the soliton equilibrium frequency reported in Fig. 4. The dashed line in Fig. 5 was obtained with the same fitting values that were used in Fig. 4.

5. CONCLUSION

In conclusion, we have investigated the self-starting nature of the Er–Yb fiber laser that includes a frequency shifter, a filter, and a nonlinear gain element, and we have characterized the soliton-train emission. The theoretical predictions for the phase width and the soliton equilibrium frequency are experimentally confirmed.

ACKNOWLEDGMENTS

The research of M. Romagnoli and W. Wabnitz was carried out under an agreement with the Italian Post and Telecommunications Administration and in the framework of a telecommunications project of the Italian National Research Council (Cosiglio Nazionale delle Ricerche). The authors thank the Australian Optical Fibre Technology Center for having provided the Er–Yb fiber and ITEL s.p.a. (Catania) for the technical support in the experiment.

REFERENCES

1. I. N. Duling III, Electron Lett. **27,** 54 (1991); D. J. Richardson, R. I. Laming, D. N. Payne, M. W. Phillips, and V. J. Mastsas, Electron. Lett. **27,** 730 (1991).
2. F. Fontana, G. Bordogna, P. Franco, M. Midrio, and M. Romagnoli, Electron. Lett. **29,** 1652 (1993).
3. P. D. Hale and F. V. Kowalski, IEEE J. Quantum Electron. **26,** 1845 (1990).
4. H. Sabert and E. Brinkmeyer, Electron. Lett. **29,** 2122 (1993).
5. F. Fontana, L. Bossalini, P. Franco, M. Midrio, M. Romagnoli, and S. Wabnitz, Electron. Lett. **30,** 321 (1994).
6. Y. Kodama, M. Romagnoli, and S. Wabnitz, Electron. Lett. **30,** 261 (1994).
7. L. F. Mollenauer, J. P. Gordon, and S. G. Evangelides, Opt. Lett. **17,** 1575 (1992).
8. Y. Kodama and S. Wabnitz, Opt. Lett. **19,** 162 (1994).
9. P. A. Belanger, J. Opt. Soc. of Am. B **8,** 2077 (1991); H. A. Haus, J. G. Fujimoto, and E. P. Ippen, J. Opt. Soc. Am. B **8,** 2068 (1991).
10. Y. Kodama, M. Romagnoli, and S. Wabnitz, Electron. Lett. **28,** 1981 (1992).
11. H. H. Chen, and C. S. Li, Phys. Rev. Lett. **37,** 693 (1976).